Substituent effects on induced current densities in penta- and heptafulvenes

Remco W. A. Havenith, Patrick W. Fowler * and Erich Steiner

School of Chemistry, University of Exeter, Stocker Road, Exeter, EX4 4QD, UK.
E-mail: P.W.Fowler@exeter.ac.uk; Fax: +44-1392-263434

Received (in Cambridge, UK) 26th October 2001, Accepted 18th January 2002
First published as an Advance Article on the web 11th February 2002

Explicit ring-current maps based on distributed-origin coupled Hartree–Fock calculations are constructed for substituted penta- and heptafulvenes C_nH_nX (n = 5, 7; X = NH_2^+, O, NH, CH_2, BH_2^-). The pattern changes from paratropic to diatropic current in the five-membered ring (*vice versa* for the seven-membered ring) as X changes from strong π electron acceptor to donor. The trend is explained by a new analysis of frontier-orbital contributions that links the currents in these substituted molecules to those in the parent carbocycle.

Introduction

Fulvenes have intrigued chemists for several decades, especially in the context of the seminal concept of aromaticity.[1–9] The properties and chemical behaviour of substituted penta- and heptafulvenes are usually rationalised in terms of their differing weights of the zwitterionic resonance structures. The relative weights of such structures depend on the electronegativity of the π-bonded substituent X, which therefore modulates the aromaticity of the ring. As the dipolar structures that possess 6 cyclic conjugated electrons (**1B** and **2A** in Scheme 1) are oppositely polarised for the five- and seven-membered rings, opposite variation of aromaticity with donor/acceptor properties of X is to be expected.

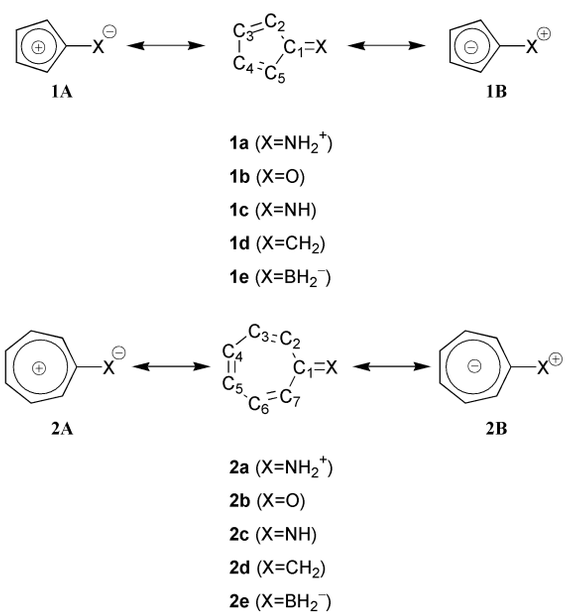

Scheme 1 The molecules under study.

The magnetic properties of a molecule serve as a probe for its aromaticity,[10–14] and, indeed, in one definition, aromaticity is defined by the ability of a ring to sustain an induced diatropic ring current. ^{1}H NMR chemical shifts of ring protons are experimental indicators of ring currents,[11] and substituted fulvenes can differ widely in this respect. The average shift [δ_{av} = (6.2 + 6.5)/2 = 6.4[3]] for the ring protons of pentafulvene (**1d**) is consistent with the absence of any significant induced ring current in this molecule. Although measured shifts are apparently not available for cyclopentadienone (**1b**), the high reactivity[1] of this species is rationalised by assuming that the electronegativity of the oxygen atom leads to the dominance of the 4π-electron resonance structure **1A** over the 6π structure **1B**, which would be expected to give a paratropic effect on ^{1}H chemical shifts. Tropone (**2b**) and the tropenylidenimmonium ion (**2a**) would appear to support diamagnetic ring currents of different strengths judging from measurements of the shifts: δ_{av} = (6.8 + 2 × 6.7)/3 = 6.7 for tropone,[15] and δ(^{1}H) for **2a** in the range 7.45–8.25,[16] which compare with an average value of 5.7[17] for the ring protons of heptafulvene (**2d**). Clearly, the nature of the substituent has a large influence on the ^{1}H NMR chemical shifts of the ring protons, and by implication, on the current density induced in the ring by an external magnetic field.

Ring currents are accessible to direct theoretical investigation using modern distributed-gauge *ab initio* methods. The objective of the present study is to use calculations of these currents to categorise the effects of electron-withdrawing/donating substituents on the induced current density in the fulvenes and to give an explanation for the observed trends in this property in terms of molecular orbital arguments. To this end, we have calculated current density maps at the coupled Hartree-Fock level of theory using the CTOCD-DZ (continuous transformation of origin of current density, diamagnetic zero) approach[18,19] for several substituted penta- and heptafulvenes (see Scheme 1). The known π systems C_5H_5X with isoelectronic π-bonded groups X = O,[20–22] NH[23] and CH_2,[24] and C_7H_7X with X = O,[12,25] CH_2,[26] NH,[27] and NH_2^+ [16,27] have substituents spanning a range of π electron-withdrawing and donating behaviour. The extremes of the hypothetical species with X = BH_2^- acting as a strong donor of π charge, and the species with X = NH_2^+ as acceptor, serve to bracket the experimentally accessible systems.

Previous studies of substituted fulvene systems[2,7–9,28,29] have mostly discussed aromaticity in terms of geometric criteria. The present visualisation of current densities points out a parallel between the magnetic and geometric criteria of aromaticity for this series; this level of agreement is not always found in ring systems.[30]

An advantage of the ipsocentric CTOCD-DZ method, in addition to its good convergence behaviour with basis size,[31] is that it allows a natural partition of the total current density into well defined orbital contributions.[32] Orbital-by-orbital analysis based on CTOCD-DZ has been successfully applied to explain, for example, the ring-current patterns in 4n *vs.* 4n + 2

 DOI: 10.1039/b109812h

Table 1 Ring bond lengths of the penta- and heptafulvenes. Bond types 1 to 3 in the pentafulvenes are {(1,2), (1,5)}, {(2,3), (4,5)} and {(3,4)}; in the heptafulvenes bond types 1 to 4 are {(1,2), (1,7)}, {(2,3), (6,7)}, {(3,4), (5,6)} and {(4,5)}. (See Scheme 1 for atom numbering)

	Bond lengths/Å			
Compound	Type 1	Type 2	Type 3	Type 4
1a (NH_2^+)	1.476	1.325	1.512	
1b (O)	1.506	1.322	1.503	
1c (NH)[a]	1.491[a]	1.326[a]	1.492	
1d (CH_2)	1.477 (1.470[b])	1.332 (1.355[b])	1.479 (1.476[b])	
1e (BH_2^-)	1.440	1.367	1.437	
2a (NH_2^+)	1.428	1.353	1.427	1.350
2b (O)	1.475 (1.445[c])	1.336 (1.364[c])	1.449 (1.462[c])	1.337 (1.342[c])
2c (NH)[a]	1.476[a]	1.333[a]	1.455[a]	1.333
2d (CH_2)	1.474 (1.450[d])	1.331 (1.365[d])	1.460 (1.470[d])	1.331 (1.344[d])
2e (BH_2^-)	1.463	1.341	1.476	1.329

[a] Average values. [b] Exp: microwave spectroscopy.[40] [c] Exp: electron diffraction.[38] [d] Exp: microwave spectroscopy.[41]

annulenes[33] and in various polycyclic systems.[32,34] It will be shown here that the empirically deduced variation of ring currents with substituent and ring size in the series **1a**–**e**, **2a**–**e** is reproduced by the computed maps and readily explained within a classical orbital picture. Ring current maps also complement and explain the trends in Nucleus Independent Chemical Shifts (NICS),[14] which are widely used as measures of aromaticity; NICS values are presented here for the two series **1a**–**e** and **2a**–**e**. Other properties diagnostic of aromatic character, which could in principle be calculated from current density, are the exaltation of magnetic susceptibility[12] and molecular magnetisability anisotropy.[13]

Methods

The geometries of all molecules were optimised at the RHF/6-31G** level, using GAMESS-UK.[35] Hessian calculations confirmed all structures as planar. **1/2a**, **b**, **d**, **e** possess the expected C_{2v} symmetry at equilibrium, and the systems **1/2c**, which contain the unsymmetrical NH group, have C_s symmetry.

Current density maps were calculated with the DZ version of the CTOCD formalism[18,19] as implemented in the SYSMO program,[36] using the 6-31G** basis set. Current densities induced by a unit magnetic field normal to the molecular plane are plotted in a standard plane $1a_0$ above that of the ring (and hence, close to the maximum π density). At this height, current flow is essentially parallel to the molecular plane. In all plots, diamagnetic (diatropic) circulation is shown anticlockwise and paramagnetic (paratropic) circulation clockwise. NICS[14] at the geometric centre of each ring were calculated using the PZ2 (paramagnetic zero)[31] variant of the CTOCD method.

Results and discussion

Geometries

The computed bond lengths for the rings are listed in Table 1. Available experimental structural data on **2b**[37–39] and **1**[40]/**2d**[41] are satisfactorily reproduced at the RHF/6-31G** level of theory, and the present results are in line with previously reported *ab initio* calculations.[7,42]

All ten systems show a pattern of bond alternation consistent with the conventional Kekulé pattern of formal single and double bonds. The alternation, as measured by the difference between average long and average short bonds, ΔR, is generally pronounced: $\Delta R = 0.17 \pm 0.02$ Å for **1a**–**d**; $\Delta R = 0.13 \pm 0.01$ Å for **2b**–**e**. The two systems that show more uniform distributions of bond lengths are **1e** ($\Delta R = 0.072$ Å), which couples the electron-deficient cyclopentadienyl ring with the electron-rich BH_2^-, and **2a** ($\Delta R = 0.076$ Å), which couples the electron-rich cycloheptatrienyl ring with the strongly electron-deficient NH_2^+ substituent. On the geometric criterion, these are therefore the two ring systems that have the most aromatic character; we will see that they are also the most aromatic on magnetic criteria. These are, of course, precisely the systems most likely to approach the zwitterionic limits **1B** and **2A** of Scheme 1.

Ring currents

Fig. 1 shows the computed π current density maps for the ten molecules. The π maps for the pentafulvene series (Fig. 1a) show a clear progression from a strong paramagnetic circulation in the five-membered ring of **1a** (X = NH_2^+), through island patterns of localised bond-centred circulations in **1c** and **1d**, to a clearly marked diamagnetic ring circulation in **1e** (X = BH_2^-). Thus, as the polarisation of the C=X bond changes, there is an accompanying reversal in direction of the ring current, as would be expected for a changeover between the limiting cases of the paramagnetic 4π-electron ring (resonance structure **1A**) and a diamagnetic ('aromatic') 6π-electron ring (**1B**). For the heptafulvenes, the trend is opposite: a diamagnetic ring current in **2a** (X = NH_2^+), is replaced by a pattern of localised islands in **2c** (X = NH) and finally a strong paramagnetic ring current in **2e** (X = BH_2^-). This is consistent with a gradual transition from the 'aromatic' 6π tropylium cation of **2A** to the 8π 'antiaromatic' anionic ring of **2B**. Both '6π' systems, **1e** and **2a**, have ring currents that are somewhat smaller than their equivalent in benzene (see inset comparison arrows, Fig. 1).

In contrast, the σ contributions to the total current density in the plotting plane are all relatively uniform superpositions of localised bond contributions, and as they add little detail to the overall picture, they will not be shown here. The total (σ + π) maps at this height above the molecular plane (Fig. 2) show more variation. In the extreme cases (**1**,**2a** and **1**,**2e**), the total map is dominated by the strong π currents. However, in **b**–**d**, where the π currents are more localised and weaker, they become hard to identify within the total, which then exhibits the typical features originating largely from σ electrons: *i.e.* an outer diamagnetic circulation around the molecular perimeter and a paramagnetic circulation over the ring centre.[43]

Chemical shifts are obtained by weighted integrations of current densities over all space and should therefore further illustrate these systematic trends. The computed NICS values of the pentafulvenes decrease monotonically from **1a** to **1e** (**1a**: +13.9, **1b**: +13.1, **1c**: +5.0, **1d**: +0.2 and **1e**: −11.1) with increasing π-donor strength of X. For the heptafulvenes, they increase along the series from **2a** to **2e** (**2a**: −6.0, **2b**: −0.3, **2c**: +1.6, **2d**: +4.5 and **2e**: +22.5). These two trends are readily understood as consequences of the opposing trends in the computed penta- and heptafulvene ring current maps (Figs. 1a and 1b). The near-zero result for **1d** is consistent with a value of −0.3 obtained with a somewhat different theoretical approach.[9]

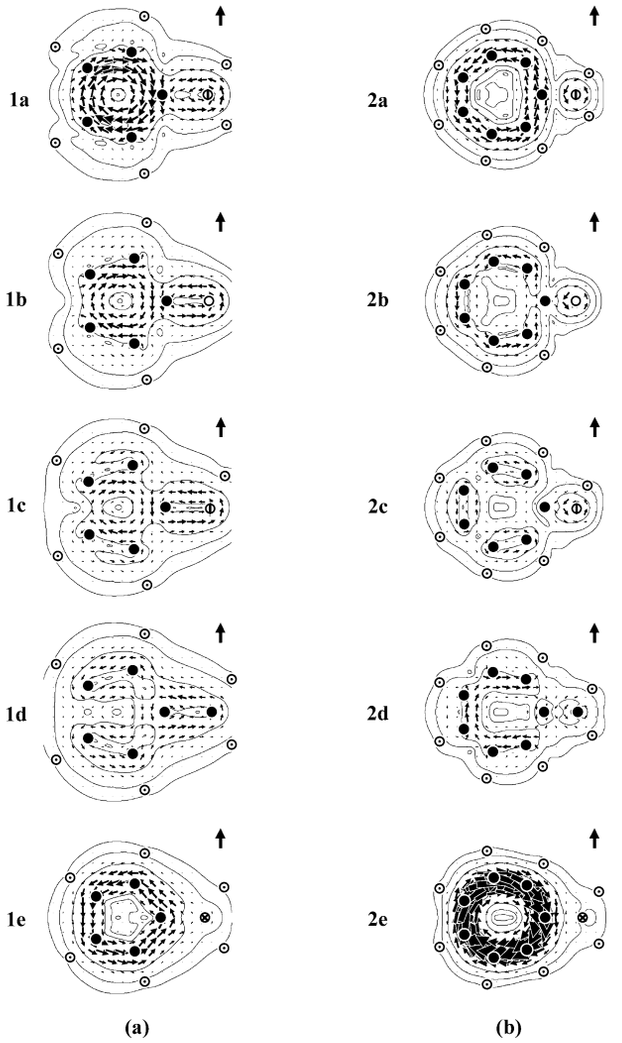

Fig. 1 Maps of π contributions to current density for (a) the substituted pentafulvenes **1a**–**e** and (b) the substituted heptafulvenes **2a**–**e**. Current densities induced by a unit magnetic field normal to the molecular plane are plotted in a plane $1a_0$ above that of the ring, with contours denoting the modulus of the current density and vectors representing in-plane projections of current. Diamagnetic (diatropic) circulation is shown anticlockwise and paramagnetic (paratropic) circulation clockwise. For comparison, an arrow indicating the maximum strength of the equivalent π-ring current in benzene is shown in the upper right corner.

The numerical values indicate a change from strongly paratropic **1a** to a system **1e** with a degree of aromaticity similar to that of benzene itself. For benzene, NICS = −12.7 in the present basis; a fully anionic cyclopentadienyl ion would have NICS = −13.8 in this basis. The heptafulvene series shows even stronger paratropicity for the strongest π-donor substituent, **2e**, as would be expected from the pronounced paratropic π current shown for this molecule in Fig. 1b.

Orbital analysis

To gain further insight into the qualitative trends that are apparent from this brief inspection of Figs. 1 and 2, it is useful to investigate the roles of individual π molecular orbitals.

In the CTOCD-DZ formalism, current density at any one point is calculated with the origin of vector potential taken at that point. It can be shown that with this so-called ipsocentric[32] choice, the total current density is a sum of orbital contributions that consist of a diamagnetic part, determined by translational virtual excitations, and a paramagnetic part, determined by rotational virtual excitations. In both parts, only transitions from occupied to unoccupied molecular orbitals are

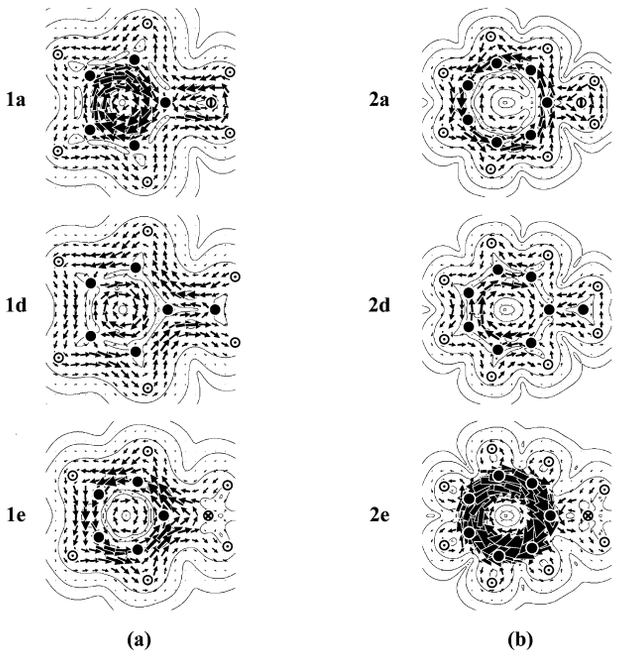

Fig. 2 Maps of total (σ + π) current density for (a) the substituted pentafulvenes **1a**, **1d** and **1e** and (b) the substituted heptafulvenes **2a**, **2d** and **2e**. The plotting plane and conventions are as in Fig. 1.

possible. The total induced current is dominated by those transitions allowed under one or both selection rules that are of low-energy, and hence usually involve electrons in frontier orbitals.

Figs. 3 and 4 show the dominant calculated orbital contributions to the π currents for pentafulvene and heptafulvene systems, respectively. These arise from two high-lying π orbitals in each case, of which one is always the HOMO. The significant orbitals include one of a_2 and one of b_1 symmetry for the C_{2v} systems and two of a″ symmetry for the C_s systems **1/2c**. In **1a**–**d**, $1a_2$ (3a″) is the HOMO. In **1a**, **1c**, **1d**, $2b_1$ (2a″) is the HOMO-1, but in **1b** it lies below a σ combination of oxygen lone-pairs and becomes the HOMO-2. In **1e**, HOMO and HOMO-1 are near-degenerate and their symmetries are swapped. In the substituted heptafulvenes **2a**–**d** the HOMO is b_1 and the HOMO-1 is a_2 (a″ in **2c**); in **2e** the HOMO-1 and HOMO-2 are near-degenerate, and the HOMO-1 corresponds to $2b_1$ and the HOMO-2 to $1a_2$. Contributions to the current in the ring from all lower-lying orbitals are small, as expected,[32,33] and are not shown here.

Several well defined trends are apparent in the dominant orbital contributions. The overall π currents in the substituted pentafulvenes are seen to result from a competition between two effects. The $1a_2$ orbital current is strongly paratropic in **1a** and weakens but remains paratropic along the series until **1d**. In contrast, the $2b_1$ orbital is diatropic throughout the series, weakly so in **1a** but increasing in magnitude until, by **1d**, the cancellation of $1a_2$ and $2b_1$ currents has produced an overall localisation of the pattern of current density. In **1e** the contribution of the $1a_2$ orbital has fully reversed, and both $1a_2$ and $2b_1$ orbitals now contribute to a diatropic ring current, resembling that arising from the 4 electrons occupying the degenerate HOMO of the isolated cyclopentadienyl anion.[33]

In the substituted heptafulvenes, the exceptional substituent is NH_2^+. For the other cases **2b**–**e**, the contribution of the $3b_1$ HOMO is paratropic, its strength increasing along the series, whilst the a_2 orbital is diatropic throughout. The exceptional **2a** has diatropic contributions from both orbitals, approaching the situation for the isolated tropylium cation, where the degenerate HOMO gives a characteristic 4-electron diatropic current.[33] The very strong paratropic circulation in **2e**, on the other hand,

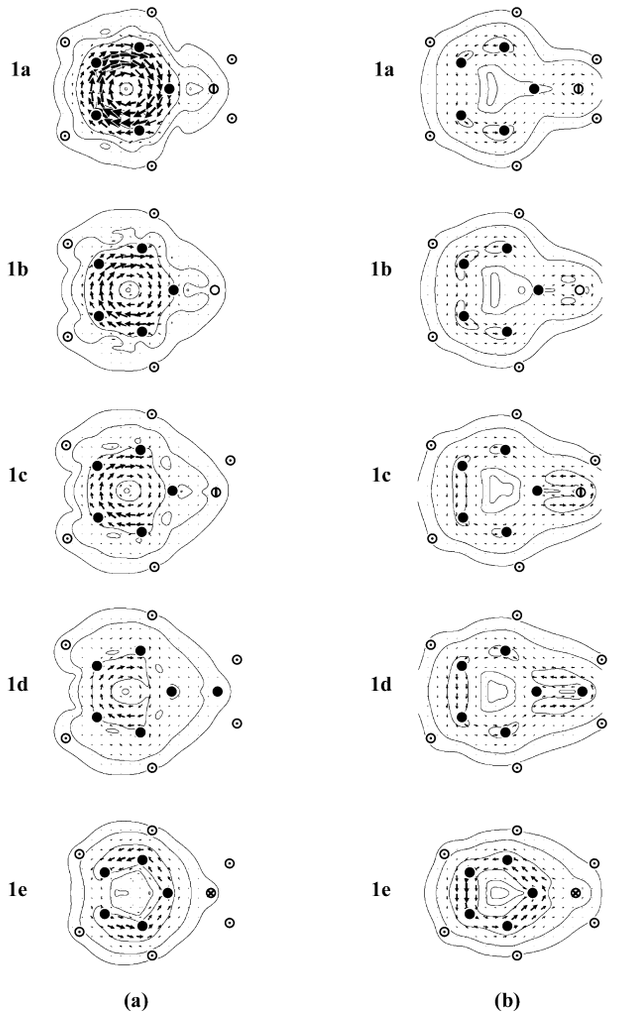

Fig. 3 Orbital contributions to the π ring currents for substituted pentafulvenes **1a**–**e**. The left hand column shows the contribution from the $1a_2$ orbital (3a″ in **1c**) and the right hand column the $2b_1$ contribution (2a″ in **1c**). Plotting conventions as in Fig. 1.

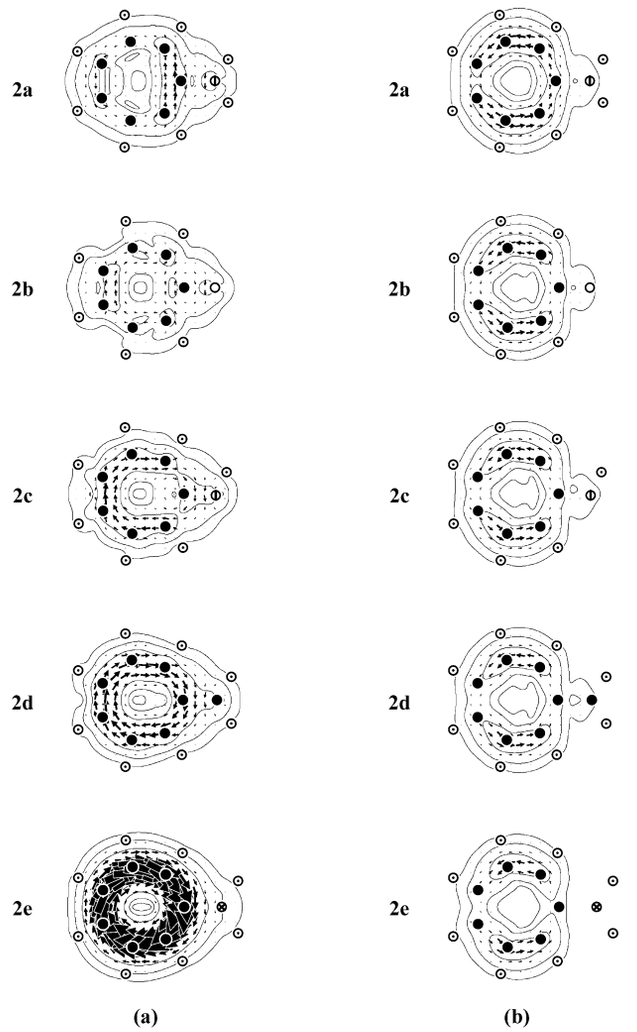

Fig. 4 Orbital contributions to the π ring currents for substituted heptafulvenes **1a**–**e**. The left hand column shows the contribution from the $3b_1$ orbital (4a″ in **2c**) and the right hand column the $1a_2$ contribution (3a″ in **2c**). Plotting conventions as in Fig. 1.

approaches the opposite limit of a 2-electron anti-aromatic ring current,[33] as found in planar cyclooctatetraene.[32]

These observations, resulting from high-level *ab initio* calculations, are all readily rationalised on qualitative electronic-structure considerations.

Electronic structure of substituted fulvenes

The essentials of the π electronic structure of substituted fulvenes can be derived from pictorial molecular orbital theory in which a substituent bearing a p_π atomic orbital is brought into interaction with the π system of the ring.

In Scheme 2, the correlation diagrams for penta- and hepta-fulvene show the π energy levels, their symmetry labels in the C_{2v} group and, for the active orbitals, pictorial representations.

Three different cases can be identified: (i) the orbital on the substituent is close in energy to the frontier orbitals of the ring, (ii) the substituent orbital is much higher in energy (X is a strong π-electron donor) or (iii) the substituent orbital is much lower in energy (X is a strong π-electron acceptor).

In the pentafulvene series, the C_{2v} symmetry leads to splitting of the degenerate π orbitals of cyclopentadienyl into a_2, b_1 pairs. In case (i), the substituent p_π orbital interacts only with the frontier b_1 component, yielding a filled $2b_1$ orbital and $3b_1$ LUMO. Since $2b_1$ is stabilised, its former partner, the $1a_2$ orbital, becomes the non-bonding HOMO in C_5H_5X. In the region of the ring, both $2b_1$ and $3b_1$ orbitals retain their nodal structure, and the energy gap is small, so that the rotationally allowed HOMO–LUMO transition $1a_2 \longrightarrow 3b_1$ is dominant. This explains the paramagnetic contribution of the HOMO to the ring current in the intermediate case.

In the extreme case (ii) of a strong π-electron donor, as in **1e**, the interaction between the b_1 HOMO of the ring and the substituent orbital is negligible, reducing the splitting between the filled $2b_1$ and $1a_2$ orbitals, and leading to an inaccessible high-energy virtual orbital centred on the substituent. The main contributions are then from the translationally allowed transitions from HOMO and HOMO-1 to their corresponding ring-centred π* orbitals, resulting in a 4-electron diamagnetic ring current, exactly as in the unsubstituted cyclopentadienyl anion.[33]

In the other extreme case (iii) of a strong π-electron acceptor, as in **1a**, it is the substituent orbital, lying well below the ring orbitals, that is doubly occupied, and the $3b_1$ virtual orbital is now ring-centred. The dominating transition is therefore the rotationally allowed $1a_2 \longrightarrow 3b_1$, across the small HOMO–LUMO gap, producing a strong paramagnetic contribution. A similar rotational transition within a symmetry-split π pair gives the general explanation of the paratropicity of the $4n$ annulenes.[33]

Analogous reasoning applies to the heptafulvenes. In the intermediate case, the HOMO/LUMO level of the ring splits into filled $3b_1$ and empty $2a_2$ levels. The $3b_1$ orbital is the rotational partner of the $2a_2$ LUMO, and the dominant $3b_1 \longrightarrow 2a_2$ excitation gives a paramagnetic HOMO contribution to the

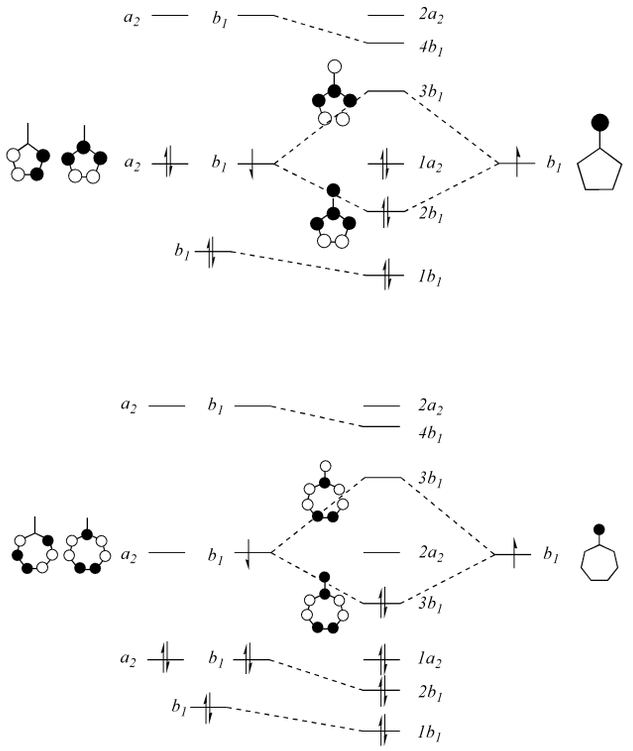

Scheme 2 Orbital interaction diagram for substituted penta- and heptafulvenes.

ring current. In the heptafulvene case, the effects of extreme donors and acceptors are reversed with respect to the pentafulvenes: the rotational transition will be favoured by a strong π-electron donor, owing to partial filling of formerly degenerate π orbitals, and the translational transition will be preferred in the case of a strong acceptor. Thus strong π-donors lead to paratropicity, strong acceptors to diatropicity in these molecules.

In fact, the predictions for continuous variation of the substituent donor/acceptor properties can be modelled in a simple way by a Hückel calculation with variable α parameter on X (Scheme 3). The change from electropositive (π-donor) to electronegative (π-acceptor) X is modelled by eqn. (1)

$$\alpha_X = \alpha_C + h_X\beta_{CC} \quad (1)$$

with h_X running from −1 to +1.[44] As the effective electronegativity of the substituent increases, the HOMO–LUMO gap in the pentafulvenes becomes smaller, because the LUMO drops in energy, while for the heptafulvenes, it is the HOMO that drops in energy, and the HOMO–LUMO gap therefore becomes larger. These changes in energy gap for the active transition modulate the current strength and correlate with the above qualitative explanation of the trends in orbital contributions. Indeed a calculation of the Hückel–London type[45,46] using the same variable-α model and an equilateral geometry for the C_n ring would give a current that goes from paramagnetic to diamagnetic at $h_X = 0.105$ ($n = 5$) and from diamagnetic to paramagnetic at $h_X = -0.059$ ($n = 7$), qualitatively accounting for both the full *ab initio* results and their orbital-based rationalisation.

Conclusions

Ab initio calculations of the induced ring currents in small odd-membered rings show pronounced substituent effects, compatible with trends in aromaticity deduced from experiment. The CTOCD-DZ approach used here gives a basis for explanation of these effects in terms of a balance of contributions to the π ring current from two frontier orbitals.

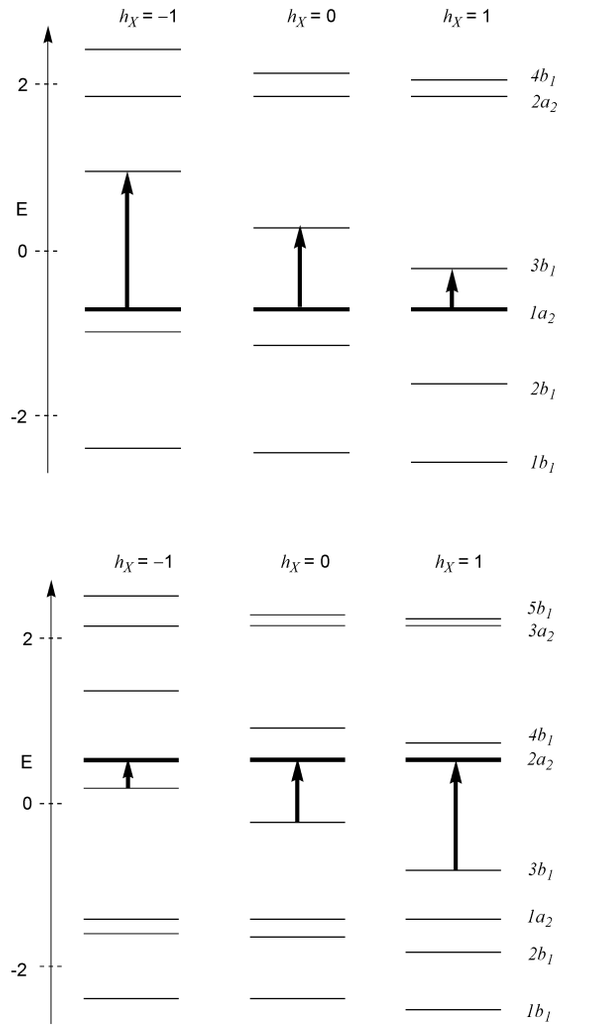

Scheme 3 Hückel energy levels for substituted five- (above) and seven-membered (below) rings C_nH_nX shown as a function of the electronegativity parameter h_X.

Orbital analysis of diatropic and paratropic contributions gives a predictive model for the opposite effects of changes in substituent π-donor strength in these rings of size $4n + 1$ and $4n + 3$, and links them in a common theoretical framework with the description of aromaticity and anti-aromaticity of pristine $4n + 2$ and $4n$ rings.

Visualisation of the *ab initio* results has given here a detailed justification for qualitative ideas based on the classical concepts of resonance theory. Similar mapping techniques interpreted on the basis of orbital symmetries and energy gaps should be applicable to a wide range of organic systems.

Acknowledgements

We thank the European Union TMR scheme, contract FMRX-CT097-0192 (BIOFULLERENES) for financial support and Professor C. J. Moody (University of Exeter) for helpful discussions.

References

1 M. A. Ogliaruso, M. G. Romanelli and E. I. Becker, *Chem. Rev.*, 1965, **65**, 261.
2 D. J. Bertelli, T. G. Andrews, Jr., and P. O. Crews, *J. Am. Chem. Soc.*, 1969, **91**, 5286.

3 R. Hollenstein, W. von Philipsborn, R. Vögeli and M. Neuenschwander, *Helv. Chim. Acta*, 1973, **56**, 847.
4 R. Hollenstein, A. Mooser, M. Neuenschwander and W. von Philipsborn, *Angew. Chem.*, 1974, **87**, 595.
5 M. Neuenschwander, *Pure Appl. Chem.*, 1986, **58**, 55.
6 M. A. McAllister and T. T. Tidwell, *J. Am. Chem. Soc.*, 1992, **114**, 5362.
7 A. P. Scott, I. Agranat, P. U. Biedermann, N. V. Riggs and L. Radom, *J. Org. Chem.*, 1997, **62**, 2026.
8 S. Saebø, S. Stroble, W. Collier, R. Ethridge, Z. Wilson, M. Tahai and C. U. Pittman, Jr., *J. Org. Chem.*, 1999, **64**, 1311.
9 W. Collier, S. Saebø and C. U. Pittman, Jr., *J. Mol. Struct. (THEOCHEM)*, 2001, **549**, 1.
10 L. Pauling, *J. Chem. Phys.*, 1936, **4**, 673.
11 J. A. Pople, *J. Chem. Phys.*, 1956, **24**, 1111.
12 H. J. Dauben, J. D. Wilson and J. L. Laity, in *Nonbenzenoid Aromatics, Vol. II*, ed. J. P. Snyder, Academic Press, New York, 1971, p. 167.
13 P. von R. Schleyer and H. Jiao, *Pure Appl. Chem.*, 1996, **68**, 209.
14 P. von R. Schleyer, C. Maerker, A. Dransfeld, H. Jiao and N. J. R. van Eikema Hommes, *J. Am. Chem. Soc.*, 1996, **118**, 6317.
15 L. A. Paquette, T. J. Watson, D. Friedrich, R. Bishop and E. Bacque, *J. Org. Chem.*, 1994, **59**, 5700.
16 M. Kato, Y. Okamoto and T. Miwa, *Tetrahedron*, 1971, **27**, 4013.
17 W. K. Schenk, R. Kyburz and M. Neuenschwander, *Helv. Chim. Acta*, 1975, **58**, 1099.
18 T. A. Keith and R. F. W. Bader, *Chem. Phys. Lett.*, 1993, **210**, 223.
19 S. Coriani, P. Lazzeretti, M. Malagoli and R. Zanasi, *Theor. Chim. Acta*, 1994, **89**, 181.
20 K. Alder and F. H. Flock, *Chem. Ber.*, 1954, **87**, 1916.
21 T. Koenig, M. Smith and W. Snell, *J. Am. Chem. Soc.*, 1977, **99**, 6663.
22 G. Maier, L. H. Franz, H.-G. Hartan, K. Lanz and H. P. Reisenauer, *Chem. Ber.*, 1985, **118**, 3196.
23 J. Morawietz and W. Sander, *Liebigs Ann. Chem.*, 1996, 2029.
24 J. Thiec and J. Wiemann, *Bull. Soc. Chim. Fr.*, 1956, 177.
25 W. von E. Doering and F. L. Detert, *J. Am. Chem. Soc.*, 1951, **73**, 876.
26 W. von E. Doering and D. W. Wiley, *Tetrahedron*, 1960, **11**, 183.
27 H. J. Dauben, Jr., and D. F. Rhoades, *J. Am. Chem. Soc.*, 1967, **89**, 6764.
28 D. J. Bertelli and T. G. Andrews, Jr., *J. Am. Chem. Soc.*, 1969, **91**, 5280.
29 T. M. Krygowski, A. Ciesielski and M. Cyranski, *Chem. Papers*, 1995, **49**, 128.
30 A. R. Katritzky, M. Karelson, S. Sild, T. M. Krygowski and K. Jug, *J. Org. Chem.*, 1998, **63**, 5228.
31 R. Zanasi, *J. Chem. Phys.*, 1996, **105**, 1460.
32 E. Steiner and P. W. Fowler, *J. Phys. Chem. A*, 2001, **105**, 9553.
33 E. Steiner and P. W. Fowler, *Chem. Commun.*, 2001, 2220.
34 E. Steiner and P. W. Fowler, *Chem. Phys. Chem.*, 2002, **3**, 114.
35 M. F. Guest, J. H. van Lenthe, J. Kendrick, K. Schöffel, P. Sherwood and R. J. Harrison, GAMESS-UK, a package of ab initio programs, with contributions from R. D. Amos, R. J. Buenker, H. J. J. van Dam, M. Dupuis, N. C. Handy, I. H. Hillier, P. J. Knowles, V. Bonačić-Koutecký, W. von Niessen, R. J. Harrison, A. P. Rendell, V. R. Saunders, A. J. Stone, D. J. Tozer and A. H. de Vries, 2000. It is derived from the original GAMESS code due to M. Dupuis, D. Spangler and J. Wendolowski, NRCC Software Catalog, Vol. 1 Program No. QG01 (GAMESS), 1980.
36 P. Lazzeretti and R. Zanasi, *SYSMO package*, University of Modena, 1980. Additional routines for evaluation and plotting of current density, E. Steiner and P. W. Fowler.
37 K. Kimura, S. Suzuki, M. Kimura and M. Kubo, *J. Chem. Phys.*, 1957, **27**, 320.
38 M. Ogasawara, T. Iijima and M. Kimura, *Bull. Chem. Soc. Jpn.*, 1972, **45**, 3277.
39 M. J. Barrow, O. S. Mills and G. Filippini, *J. Chem. Soc., Chem. Commun.*, 1973, 66.
40 P. A. Baron, R. D. Brown, F. R. Burden, P. J. Domaille and J. E. Kent, *J. Mol. Spectrosc.*, 1972, **43**, 401.
41 A. Bauder, C. Keller and M. Neuenschwander, *J. Mol. Spectrosc.*, 1976, **63**, 281.
42 N. Sanna, F. Ramondo and L. Bencivenni, *J. Mol. Struct.*, 1994, **318**, 217.
43 E. Steiner and P. W. Fowler, *Int. J. Quantum Chem.*, 1996, **60**, 609.
44 A. Streitwieser, Jr., *Molecular Orbital Theory for Organic Chemists*, John Wiley & Sons Inc., New York, 1962.
45 F. London, *J. Phys. Radium*, 1937, **8**, 397.
46 A. Pasquarello, M. Schlüter and R. C. Haddon, *Phys. Rev. A*, 1993, **47**, 1783.